Journal of Mechatronics, Electrical Power, and Vehicular Technology 17 (2026) 194-205

Journal of Mechatronics, Electrical Power, and Vehicular Technology

e-ISSN: 2088-6985
p-ISSN: 2087-3379

mev.brin.go.id

Adaptive PID control using TSK elliptic fuzzy and static feedforward for observable disturbance rejection in industrial heating ovens

Ali Rospawan [a], Clara Lavita Angelina [a, *], I Made Andik Setiawan [a], Zanu Saputra [a], Ocsirendi [a], Aan Febriansyah [a], Indra Dwisaputra [a], Dedy Ramdhani Harahap [b]

[a] *Department of Electronics Engineering, Politeknik Manufaktur Negeri Bangka Belitung*
[b] *Department of Mechanical Design Politeknik Manufaktur Negeri Bangka Belitung*
Kawasan Industri Air Kantung, Sungailiat, 33215, Indonesia

Abstract

This paper presents an advanced control strategy aimed at accelerating the temperature recovery time in industrial heating ovens, particularly in response to observable disturbances such as periodic door openings. The proposed method combines a Takagi-Sugeno-Kang (TSK) elliptic fuzzy-based adaptive proportional-integral-derivative (PID) control with a static feedforward (FF) control strategy. The TSK elliptic fuzzy system models the input-output dynamics and adaptively adjusts the PID gains, allowing the controller to respond effectively to varying system conditions. The static feedforward control is designed to specifically counteract the measurable disturbances to shorten recovery time and improve stability. The strategy is validated through both simulation and experiment on a low-cost STM32 microcontroller. Compared with a conventional PID controller, it reduced the RMSE by 32.27 % and the ISE by 54.13 %, together with a recovery time shortened by approximately 72 s, reflecting the faster disturbance recovery achieved by the static feedforward action. Experimental results confirmed these findings, with a higher feedforward gain further reducing the temperature drop and accelerating recovery. The proposed technique offers a reliable and practical solution for practitioners in managing similar disturbance patterns in industrial settings.

Keywords: adaptive proportional-integral-derivative (PID); elliptic membership function; feedforward (FF) control; heating oven; Takagi-Sugeno-Kang (TSK) fuzzy.

I. Introduction

Industrial heating ovens play a critical role in various manufacturing processes, including heat-treating metals, curing coatings, baking, and, more importantly, the semiconductor packaging industry. Maintaining precise temperature control in the presence of disturbances is crucial for product quality, process efficiency, and ensuring that products receive the correct temperature exposure for the required duration. A particularly common and impactful disturbance in industrial settings is the periodic opening of oven doors for loading or unloading materials, which introduces a sudden and significant thermal drop [1]. Although such door-opening events are predictable and measurable, they can cause prolonged temperature recovery times, energy inefficiency, and potential quality degradation in the processed materials [2][3].

* Corresponding Author. clara_lavita_angelina@polman-babel.ac.id (C. L. Angelina)

https://doi.org/10.55981/j.mev.2026.1094

Received 21 August 2025; revised 6 May 2026; accepted 1 July 2026; available online 31 July 2026; published 31 July 2026

How to Cite: A. Rospawan *et al.*, "Adaptive PID control using TSK elliptic fuzzy and static feedforward for observable disturbance rejection in industrial heating ovens," *Journal of Mechatronics, Electrical Power, and Vehicular Technology*, vol. 17, no. 1, pp. 194-205, July, 2026.

Proportional-integral-derivative (PID) control remains the dominant solution for industrial temperature regulation owing to its simplicity, robustness, and ease of implementation, and continues to serve as the baseline upon which modern tuning and optimization schemes are built [4]. However, conventional PID control suffers from two limitations. First, fixed PID gains involve an inherent trade-off, namely, an excessive proportional or integral gain causes overshoot and oscillation, while insufficient gain results in slow response and persistent steady-state error. Similarly, excessive derivative gain amplifies measurement noise, while insufficient derivative gain fails to damp the transient response [5]. Second, and more fundamentally, PID is purely a reactive feedback mechanism, in which it can only respond to a disturbance after the resulting error has already appeared at the output. For a heating oven with large thermal inertia and a long-time delay, this reactive nature inherently limits how quickly the temperature can recover after a door-opening event, regardless of how well the gains are tuned.

To address the first limitation, considerable research effort has been devoted to adaptive and intelligent PID strategies that adjust the controller gains online, with fuzzy logic in particular proving practical even on resource-constrained embedded platforms. The authors in [6] proposed a differential-evolution-based adaptive fuzzy PID controller that dynamically adjusts the control parameters in response to changing conditions in a continuous stirred tank reactor (CSTR), effectively handling process nonlinearities and uncertainties. However, the gain adaptation is driven solely by the feedback error, and the controller therefore still reacts only after a disturbance has propagated to the output, and no mechanism exploits prior knowledge of a recurring disturbance. Similarly, an improved particle swarm optimization-based fuzzy PID (IPSO-PID) algorithm was introduced in [7] to overcome the inadequate adaptability and slow response of conventional temperature control, demonstrating clear improvements in adaptability and response time. Nevertheless, population-based optimization such as PSO imposes a considerable computational burden that is poorly suited to low-end microcontrollers [8], and, like [6], the scheme remains a pure feedback structure with no anticipatory action against known disturbances.

To overcome the reactive nature of feedback-only structures, several studies have integrated feedforward (FF) action with PID-type controllers. A feedforward-augmented load frequency controller for microgrids was proposed in [9], in which disturbances estimated by a disturbance observer are compensated in a feedforward path, reducing frequency-deviation criteria. The effectiveness of [9], however, depends on the accuracy and convergence of the disturbance observer, which adds design complexity and computational load that may be unnecessary when the disturbance is directly measurable. The authors in [10] combined an intelligent-PID controller with a PD feedforward term to improve trajectory tracking of an autonomous underwater vehicle under complex disturbances, significantly outperforming traditional PID; yet the feedforward term is derived from the reference trajectory rather than from an exogenous disturbance signal, so the approach does not directly transfer to disturbance rejection in thermal processes. Closer to the present work, static feedforward terms injected directly into fuzzy-based PID loops were proposed in [11] and [12] for the air-supply and hydrogen-pressure subsystems of vehicular fuel cells, improving dynamic response and stability. These studies confirm the practical value of static feedforward compensation. However, they address fast electrochemical/pneumatic dynamics rather than slow, long-time-delay thermal dynamics, and neither combines the feedforward action with an online-adapting PID whose gains are tuned by a learned model of the plant.

From these recent studies, it is evident that existing adaptive intelligent PID schemes improve gain tuning and transient response but remain purely reactive and mostly not suitable for low-end hardware. To the best of our knowledge, no prior work has combined a static feedforward compensator, triggered directly by a door-state sensor and sized analytically from the thermal energy balance, with an online TSK elliptic fuzzy-based adaptive PID controller implemented on a low-end microcontroller, for fast temperature recovery in industrial heating ovens subject to periodic door openings.

Accordingly, this paper proposes an enhanced control strategy that integrates TSK elliptic fuzzy-based adaptive PID control with static feedforward compensation. The PID controller serves as the main feedback controller, and the TSK elliptic fuzzy identification system models the oven's input-output dynamics online and adaptively adjusts the PID gains, accelerating the otherwise slow transient response while maintaining stability at the desired setpoint. The static feedforward path, activated by the door-state signal, anticipates the thermal loss caused by door openings and preemptively injects the compensating control effort, thereby shortening the recovery time well beyond what feedback action alone can achieve. The TSK elliptic membership function is adopted over conventional triangular or Gaussian forms because its wider, elliptical support has been shown to handle noise and nonlinearity more effectively, offering a more flexible and robust representation of uncertainty under parameter variation and external disturbance [13]. By capturing a broader range of input data with enhanced membership-degree shapes, TSK elliptic fuzzy systems can deliver more accurate control actions and better overall stability [14].

The objectives of this study are fourfold. First, a comprehensive model of an industrial heating oven is developed as a first-order time-delay (FOTD) system, accounting for observable disturbances in the form of periodic door openings. Second, an integrated control strategy combining static feedforward control with TSK elliptic fuzzy-based adaptive PID control is designed to maintain temperature stability and accelerate disturbance recovery across a range of operating conditions. Third, the proposed control system is implemented in a real-time embedded environment based on an STM32 microcontroller and evaluated under continuous production scenarios. Finally, a comparative analysis is performed against conventional PID control, TSK fuzzy-based, and elliptic fuzzy-based adaptive PID control (with and without feedforward), in terms of maximum error, root mean square error (RMSE), integral of squared error (ISE), integral of absolute error (IAE), integral of time-weighted absolute error (ITAE), and recovery time, through both simulation and experimental validation [15][16].

The rest of this paper is organized as follows, section II presents the system specifications, modeling, and design of the adaptive PID control system with TSK elliptic fuzzy logic and static feedforward control; section III discusses the validation of the proposed method through simulation and experimental analysis, focusing on temperature stability and recovery-time improvement. Finally, section IV provides the conclusion, summarizing the findings and outlining directions for future research.

II. Materials and Methods

In section II, the experimental setup and control design methodologies used to implement the proposed static feedforward control strategy for the industrial heating oven, including a comprehensive overview of the system's configuration, materials, design of the controller, and the industrial heating oven system modeling, are presented in detail.

A. System specification and modeling of industrial heating oven

In this paper, the utilization of a static feedforward control strategy as a compensator for the observable and measurable disturbances that arise from periodic door openings in industrial heating ovens is proposed. To design and implement such a system effectively, it is essential to first clarify the list of components, parameters, and specifications of the experimental testbed (Figure 1). The physical layout of the heating

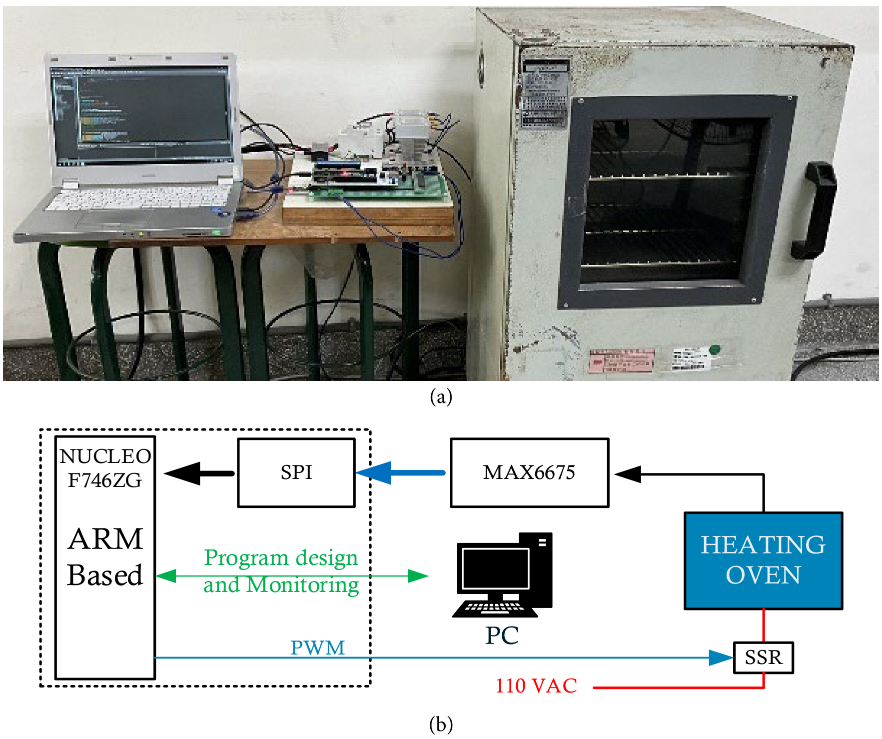

Figure 1. Industrial heating oven testbed: (a) physical experimental setup, from left to right showing: the laptop computer, the power and control board, and the heating oven; and (b) schematic control diagram.

Table 1.
Heating oven operational specification.

Parameter	Value
Working temperature	40 to 250 °C
Working voltage	110 V AC
Maximum load current	8 A
Desired setpoint (r)	150 °C
Heating chamber volume (v)	0.027 m^3 (cube 0.3 m)
Air density (ρ)	0.834 kg/m^3
Heat capacity of air (cp)	1018 J/(kg.°C)
Maximum power ($P_{\max}$)	500 W
Expected temperature drop (ΔT)	45 °C at 30 s of door opening
Expected recovery time (t_{recovery})	60 s maximum

oven used in the experiments is illustrated in Figure 1(a), while Figure 1(b) provides the hierarchical schematic control diagram.

The experimental setup includes several key components. The STM32-F746ZG microcontroller board serves as the main control unit, executing the control algorithms and interfacing with other system components. A solid-state relay (FOTEK SSR-25 DA) functions as the switching device that converts the pulse-width modulation (PWM) signals that operate at a frequency of 1 Hz with a flexible duty cycle range of 0 to 100 %, which regulates the single-phase power of a 110 V AC signal for the heating element in the oven. Temperature measurements are facilitated by a MAX6675 thermocouple-to-digital converter, which interfaces with a K-type thermocouple and transmits temperature data to the STM32 microcontroller via the serial peripheral interface (SPI) protocol. Additionally, a computer is utilized for program design, system monitoring, and data logging, ensuring a comprehensive approach to system control and performance evaluation. The specific parameters critical for understanding the energy conversion dynamics of the industrial heating oven are detailed in Table 1.

Furthermore, building on the system modeling approaches [2][17], the industrial heating oven was modelled using the FOTD system. This type of model is particularly suitable for capturing the dynamics of systems where there is a significant time delay between the input and output response, as it's a common characteristic in thermal systems [18]. The system transfer function in the continuous-time domain $G(s)$ is represented in equation (1):

$$G(s) = \frac{K_P}{1+T_{p1}s}\exp(-T_d s) = \frac{294.18}{1+2760.9s}\exp(-327.88s) \quad (1)$$

where K_P is the process gain, T_{p1} is the time constant, T_d is the time delay, and s is the Laplace variable [19].

To facilitate digital control, this continuous-time model is discretized. The discrete-time model, derived using a sampling time of 6 s, allows for the implementation of control algorithms in the STM32 microcontroller. The choice of a 6-second sampling interval balances the trade-off between control responsiveness and computational load, ensuring the system can react effectively to disturbances while maintaining real-time performance.

The FOTD model's parameters are critical for accurately predicting the system's response to control inputs and disturbances. By precisely characterizing the heating oven's dynamic behavior, we can tailor the feedforward control strategy to counteract the effects of door openings, thereby minimizing temperature fluctuations and improving process stability. This modeling approach not only aids in controller design but also serves as a foundation for simulation studies, which are integral to validating the proposed control strategy before experimental implementation.

B. TSK elliptic fuzzy-based identification system

The identification of dynamic systems in complex environments requires a flexible and adaptive approach to model system behavior accurately. The TSK elliptic fuzzy-based identification system serves as a highly effective tool to capture nonlinear system dynamics by establishing a set of fuzzy rules that guide the system's input-output relationship. By utilizing elliptic fuzzy membership functions and adaptive weight updating mechanisms, the model continuously adjusts to real-time changes in system behavior, enabling more accurate predictions and control responses. This approach not only enhances system stability but also improves the performance of the feedforward and PID control strategies by providing a more reliable system model.

1) System identification design using TSK elliptic fuzzy

In designing a system identification framework that accurately captures the system's dynamic relationship between input and output, the modeling of the system is defined in equation (2):

$$y(k+1) = f\left(y(k), \cdots, y\left(k-n_y\right), u(k), \cdots, u(k-n_u)\right) \quad (2)$$

where f represents the function that models the system's dynamics based on the system output y at the current sampling instance and up to n_y number of previous system outputs, as well as the system input u

at the current instance and up to n_u number of previous system inputs. This equation captures the system's behavior over time by incorporating historical data from both inputs and outputs.

To characterize the system's dynamics using fuzzy logic, we establish fuzzy rules within a Takagi-Sugeno-Kang (TSK) fuzzy framework. For a system with M fuzzy input variables, where each fuzzy subsystem i has K_i fuzzy rules, the typical TSK fuzzy rule can be expressed as equation (3):

if x_{s1} is A_{k1}^i and x_{s2} is A_{k2}^i and $\cdots$ and x_{sM} is A_{kM}^i then $z_k^i = f_k^i(x_{s1}, x_{s2}, \cdots, x_{sM}), k = 1,2,\cdots,K_i$ (3)

where f_k^i denotes the function that models the system input $x_{s1}, x_{s2}, \cdots, x_{sM}$ associated with $A_{k1}^i \cdots A_{kM}^i$ of the fuzzy sets. Then, the output z_{sk}^i of a given rule is computed by equation (4):

$$z_{sk}^i = f_k^i(x_{s1}, x_{s2}, \cdots, x_{sM}) = \sum_{l=1}^{M} \alpha_{kl}^i x_{sl} \tag{4}$$

where α_{kt}^i are coefficients randomly generated from a uniform distribution in the range [0,1]. Note that in some cases, these coefficients might be constrained to a narrower range, such as [0,0.1], to ensure stability and better fitting [20].

The firing strength of the k^{th} fuzzy rule in the i^{th} fuzzy subsystem is given by equation (5):

$$\tau_{sk}^i = \prod_{l=1}^{M} \mu_{kl}^i(x_{sl}) \tag{5}$$

where $\mu_{kl}^i(x_{sl})$ represents the membership function value of the l^{th} input x_{sl} in the i^{th} fuzzy set A_{kl}^i. To normalize firing strength, equation (6) is calculated:

$$\lambda_{sk}^i = \frac{\tau_{sk}^i}{\sum_{k=1}^{K_i} \tau_{sk}^i} \tag{6}$$

The elliptic membership function used to compute μ_{kl}^i is defined in equation (7):

$$\mu_{kt}^i = \begin{cases} \left(1 - \left|\frac{x - c_{kt}^i}{\sigma_{kt}^i}\right|^{q_{kt}^i}\right)^{\frac{1}{q_{kt}^i}}, & \left|\frac{x - c_{kt}^i}{\sigma_{kt}^i}\right| < 1 \\ 0, & \text{others} \end{cases} \tag{7}$$

where c_{kl}^i and σ_{kl}^i are the elliptic membership degree center and width parameters. This formulation ensures that the membership degree is computed only within the defined range to simplify calculations and reduce computational complexity [13][21]. Finally, the output of the TSK elliptic fuzzy system is computed by equation (8):

$$\hat{y} = \sum_{i=1}^{n} \sum_{k=1}^{K_i} \lambda_{sk}^i w_k^i \left(\sum_{l=1}^{M} \alpha_{kl}^i x_{sl}\right) \tag{8}$$

where w_k^i represents the weight associated with the k^{th} fuzzy rule in the i^{th} fuzzy subsystem and $\hat{y}$ is the system output estimate.

2) Parameter updating algorithm

To optimize the system response, we employ an error objective function that focuses on minimizing the discrepancy between the predicted and actual system outputs. The objective function is defined in equation (9):

$$E(k) = \frac{1}{2}\left(\hat{y}(k) - y(k)\right)^2 \tag{9}$$

where $\hat{y}(k)$ denotes the predicted system output, and $y(k)$ represents the actual system response at sampling instance k. The goal is to adjust the weight parameters of the TSK elliptic fuzzy system to minimize this error function, thus improving the accuracy of the system identification. Then, the weights of the TSK elliptic fuzzy can be computed by equation (10):

$$\begin{cases} w_k^i(k+1) = w_k^i(k) - \eta(k)\frac{\partial E}{\partial w_k^i} \\ c_{kt}^i(k+1) = c_{kt}^i(k) - \eta(k)\frac{\partial E}{\partial c_{kt}^i} \\ \sigma_{kt}^i(k+1) = \sigma_{kt}^i(k) - \eta(k)\frac{\partial E}{\partial \sigma_{kt}^i} \end{cases} \tag{10}$$

where $\eta(k)$ represents the learning rate at sampling instance k. As the $\partial E/\partial \hat{y} = \hat{y} - y = \hat{e}$, then we obtain equation (11) to equation (13):

$$\frac{\partial E}{\partial w_k^i} = \frac{\partial E}{\partial \hat{y}} \cdot \frac{\partial \hat{y}}{\partial w_k^i} = (\hat{y} - y) \cdot \lambda_k^i \left(\sum_{l=1}^{M} \alpha_{kl}^i x_{sl}\right) \tag{11}$$

$$\frac{\partial E}{\partial c_{kl}^i} = \frac{\partial E}{\partial \hat{y}} \cdot \frac{\partial \hat{y}}{\partial c_{kl}^i} = (\hat{y} - y) \cdot \sum_{i=1}^{n} \sum_{k=1}^{K_i} \lambda_{sk}^i \left(\sum_{l=1}^{M} \alpha_{kl}^i x_{sl}\right) \cdot \frac{2\left(x - c_{kt}^i\right)}{\left(\sigma_{kt}^i\right)^2} \tag{12}$$

$$\frac{\partial E}{\partial \sigma_{kl}^i} = \frac{\partial E}{\partial \hat{y}} \cdot \frac{\partial \hat{y}}{\partial \sigma_{kl}^i} = (\hat{y} - y) \cdot \sum_{i=1}^{n} \sum_{k=1}^{K_i} \lambda_{sk}^i \left(\sum_{l=1}^{M} \alpha_{kl}^i x_{sl}\right) \cdot \frac{2\left(x - c_{kt}^i\right)^2}{\left(\sigma_{kt}^i\right)^3} \tag{13}$$

C. Adaptive PID with static feedforward control

The combination of an adaptive PID controller with a static feedforward control strategy offers a powerful solution for managing known and measurable disturbances in industrial processes. The adaptive PID controller provides a real-time adjustment of the proportional, integral, and derivative gains to respond dynamically to variations in the process. On the other hand, the static feedforward control leverages known disturbances, such as periodic door openings in the heating oven, to preemptively counteract their effects. By integrating both control strategies, the system is able to maintain temperature stability and minimize recovery time, ensuring optimal performance even in challenging operating conditions. The following sections outline the design and implementation of both controllers.

1) Adaptive PID controller design

PID control is a fundamental approach in industrial automation, renowned for its simplicity and effectiveness [22]. In the context of temperature control for heating ovens, the PID algorithm calculates the control output $u(k)$ based on the error $e(k)$ between the setpoint $r(k)$ and the measured temperature $y(k)$. The discrete time PID control law is expressed as equation (14):

$$u_{\text{PID}}(k) = k_P \cdot e(k) + k_I \cdot \Delta e(k) + k_D \cdot \Delta^2 e(k) \quad (14)$$

where k_P represent the proportional gain, k_I the integral gain and k_D is the derivative gain. Each term in the PID control law has a specific role: the proportional term $k_P \cdot e(k)$ provides an immediate response to the current error; the integral term $k_I \cdot \Delta e(k)$ eliminates steady-state error, and the derivative term $k_D \cdot \Delta^2 e(k)$ improves transient response [23][24]. The errors used in the control calculation are defined in equation (15):

$$\begin{cases} e(k) = r(k) - y(k) \\ \Delta e(k) = e(k) - e(k-1) \\ \Delta^2 e(k) = e(k) - 2\big(e(k-1)\big) + e(k-2) \end{cases} \quad (15)$$

where $\Delta e(k)$ represents the first derivative of the error and $\Delta^2 e(k)$ is the second derivative of the error in discrete time.

As the PID system is proposed to be adaptive, the system cost function is defined to optimize the controller parameters, with details written in equation (16):

$$J(k) = \frac{1}{2}\big(r(k) - \hat{y}(k)\big)^2 \quad (16)$$

Then, as the system receives the PID gains adjustment from the adaptive identification system, the gains are adjusted based on the cost function (equation (16)), and the following update rules are written in equation (17):

$$\begin{cases} k_P(k+1) = k_P(k) + \Delta k_P(k) = k_P(k) - \eta_c \frac{\partial J(k)}{\partial k_P(k)} \\ k_I(k+1) = k_I(k) + \Delta k_I(k) = k_I(k) - \eta_c \frac{\partial J(k)}{\partial k_I(k)} \\ k_D(k+1) = k_D(k) + \Delta k_D(k) = k_D(k) - \eta_c \frac{\partial J(k)}{\partial k_D(k)} \end{cases} \quad (17)$$

where η_c is the adaptive PID controller learning rate. Furthermore, the gradients of the cost function with respect to the PID parameters are derived in equation (18):

$$\begin{cases} \frac{\partial J(k)}{\partial k_P(k)} = \frac{\partial J(k)}{\partial \hat{y}(k)} \frac{\partial \hat{y}(k)}{\partial \Delta u(k)} \frac{\partial \Delta u(k)}{\partial k_P(k)} \\ \frac{\partial J(k)}{\partial k_I(k)} = \frac{\partial J(k)}{\partial \hat{y}(k)} \frac{\partial \hat{y}(k)}{\partial \Delta u(k)} \frac{\partial \Delta u(k)}{\partial k_I(k)} \\ \frac{\partial J(k)}{\partial k_D(k)} = \frac{\partial J(k)}{\partial \hat{y}(k)} \frac{\partial \hat{y}(k)}{\partial \Delta u(k)} \frac{\partial \Delta u(k)}{\partial k_D(k)} \end{cases} \quad (18)$$

where $\frac{\partial J(k)}{\partial \hat{y}(k)} = \big(r(k) - \hat{y}(k)\big)$, $\frac{\partial \Delta u(k)}{\partial k_P(k)} = \Delta e(k)$, $\frac{\partial \Delta u(k)}{\partial k_I(k)} = e(k)$, and $\frac{\partial \Delta u(k)}{\partial k_D(k)} = \Delta^2 e(k)$.

2) Static feedforward controller design

PID control alone may not adequately handle the rapid disturbances caused by periodic door openings in industrial ovens. To overcome this issue, an effective static feedforward control is proposed as a proactive control strategy that leverages this periodic and measurable disturbance information to anticipate and counteract their effects before they significantly impact the process variable. The core principle involves modeling the expected disturbance, which in this case is the temperature drop due to the door opening, and applying a pre-calculated compensatory action in addition to the PID control output. This action enhances the system's ability to maintain desired temperature levels and reduce temperature recovery time despite having disturbances.

To implement static feedforward control, we first model the expected temperature drops ΔT due to door openings by equation (19):

$$\Delta T = T_{\text{setpoint}} - T_{\text{measured after the door opened}} \quad (19)$$

where $T_{\text{setpoint}} = r(k)$ is the target temperature and $T_{\text{measured after the door opened}}$ is the temperature immediately after the door has been opened. The heat energy Q required to compensate for the temperature drop can be calculated using equation (20):

$$Q = m \cdot cp \cdot \Delta T \quad (20)$$

where m is the effective mass of air in the oven, obtained from the product of the oven volume v and the air density ρ, and cp is the specific heat capacity of air [25]. Then, the feedforward power P_{FF} is computed by computing equation (21):

$$P_{FF} = \frac{Q}{t_{\text{recovery}}} \quad (21)$$

where t_{recovery} is the desired recovery time that can be adjusted as quickly as possible, depending on the heater's capabilities.

Furthermore, the feedforward control output u_{FF} can be expressed as equation (22):

$$u_{FF} = K_{FF} \times \left(\frac{P_{FF}}{P_{\max} \times P_{\text{coef}}}\right) \quad (22)$$

where $P_{\max}$ is the maximum power output of the heating oven, P_{coef} is the coefficient efficiency of maximum power delivered by the heating oven and K_{FF} is the gain factor used to amplify the feedforward effect. Typically, $10 \leq K_{FF} \leq 20$ is a suitable range, but it may be adjusted based on the desired system response. It is also important to note that the gain factor

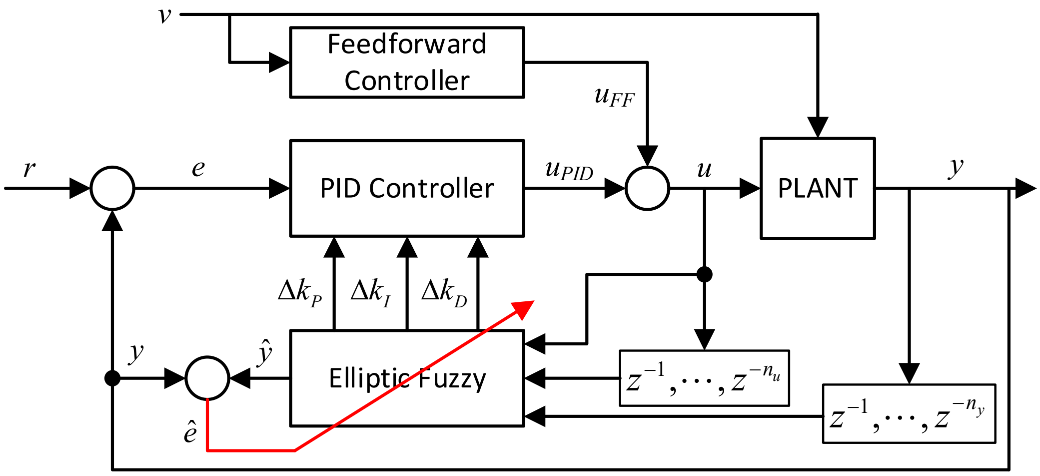

Figure 2. Static feedforward with TSK elliptic fuzzy-based adaptive PID closed-loop diagram.

K_{FF} may become negative if the disturbance leads to an increase in the system response or an overshoot-like form, depending on the system being controlled.

3) Integrationf of static feedforward and adaptive PID controller

To achieve optimal system performance, the overall system control output $u(k)$ is calculated by combining the PID control output (equation (14)) and the feedforward control output (equation (22)) by computing equation (23):

$$u(k) = u_{\mathrm{PID}}(k) + u_{FF}(k) \tag{23}$$

During normal operation with the door state in a closed condition, the feedforward controller output u_{FF} will become zero, and when the door state is in the open condition, equation (22) is computed until the door is closed, and the length of the compensation time FF_{Duration} is achieved. Furthermore, the closed-loop configuration of the proposed static feedforward with TSK elliptic fuzzy-based adaptive PID control structure is illustrated in Figure 2.

4) Real-time control algorithm

To ensure optimal system performance, the real-time control algorithms of the proposed static feedforward adaptive PID control approach are outlined as written in Algorithm 1.

Algorithm 1 Static Feedforward Adaptive PID Control.

Input System error $e(k)$, door sensor status.
Output Combined controller output $u(k)$.

Initialize the gains of K_P, K_I, K_D and FF_{Duration}
Initialize the TSK elliptic fuzzy weight parameters
For $k = 1$ to K (total sampling number)
  Calculate the error $e(k)$
  Calculate PID control output $u_{\mathrm{PID}}(k)$
    if doorState == OPEN:
      $u_{FF}(k) = K_{FF} * (P_{FF}/(P_{\max} * P_{\mathrm{coef}}))$
      doorOpenTime $= k$
    else if $k -$ doorOpenTime $< FF_{\mathrm{Duration}}$:
      $u_{FF}(k) = K_{FF} * (P_{FF}/(P_{\max} * P_{\mathrm{coef}}))$
    else:
      $u_{FF}(k) = 0$
    end if
  Compute $u(k) = u_{\mathrm{PID}}(k) + u_{FF}(k)$
  Calculate the TSK elliptic fuzzy inputs (equation (2))
  Calculate the TSK elliptic fuzzy output (equation (8))
  Perform fuzzy weight updates (equation (10))
  Adjust the next iteration of PID gains (equation (17))
End

III. Results and Discussions

In section III, the performance of the proposed control strategy is analyzed through both simulation and experimental validation. The results provide a comprehensive comparison with existing control methods, highlighting the improvements achieved by integrating feedforward control with adaptive PID and TSK elliptic fuzzy-based techniques. The simulations demonstrate significant enhancements in setpoint tracking, recovery time, and error reduction, particularly in response to disturbances caused by door openings in the industrial heating oven. Experimental results further corroborate these findings, showing that higher feedforward gains lead to faster recovery and improved temperature stability, albeit with a slight risk of overshoot.

A. Simulational validation

Using the oven specifications in Table 1, the feedforward power required to compensate for the door-opening temperature drop is obtained from equation (20) and equation (21) as $P_{FF} = 17.1925$ W. Substituting this into equation (22), with $P_{\max} =$ 500 W and $P_{\mathrm{coef}} = 0.9$, gives a feedforward control output of $u_{FF} = K_{FF} \times 3.8205$ %. For the simulation,

Table 2.
Controller performance comparison.

Controller	Max Error	RMSE	ISE	IAE	ITAE
Conventional PID	27.1501	4.4367	39368	3100.4	3063400
TSK fuzzy PID (no FF)	22.8915	3.7803	28581	2855.5	2777900
Elliptic fuzzy PID (no FF)	22.8701	3.7527	28166	2821.8	2713700
TSK fuzzy PID (with FF)	20.8145	3.0324	18391	2179.6	1944000
Elliptic fuzzy PID (with FF)	20.5537	3.0051	18060	2151.8	1903400

Table 3.
Controller performance improvement percentage over conventional PID.

Controller	Max Error	RMSE	ISE	IAE	ITAE
TSK fuzzy PID (no FF)	↑ 15.69 %	↑ 14.79 %	↑ 27.40 %	↑ 7.90 %	↑ 9.32 %
Elliptic fuzzy PID (no FF)	↑ 15.76 %	↑ 15.42 %	↑ 28.45 %	↑ 8.99 %	↑ 11.42 %
TSK fuzzy PID (with FF)	↑ 23.34 %	↑ 31.65 %	↑ 53.28 %	↑ 29.7 %	↑ 36.54 %
Elliptic fuzzy PID (with FF)	↑ 24.30 %	↑ 32.27 %	↑ 54.13 %	↑ 30.6 %	↑ 37.87 %

$K_{FF} = 10$ was selected, resulting in $u_{FF} = 38.205$ %. The initial PID gains were set as $k_P = 0.3$, $k_I = 0.002$ and $k_D = 1.5$, with learning rates $\eta = \eta_c = 0.001$. The duration of the feedforward control action FF_{Duration} was set to eight sampling instances, or three sampling instances after the door state is closed.

Furthermore, Table 2 presents a comparative analysis of the controller performance with its improvements in Table 3 achieved from the simulation result of five different controllers namely: conventional PID control, TSK fuzzy-based adaptive PID control without the addition of feedforward control [26], TSK elliptic fuzzy-based adaptive PID without the addition of feedforward control, static feedforward control with TSK fuzzy-based adaptive PID control, and the proposed static feedforward control with TSK elliptic fuzzy-based adaptive PID control. The results clearly demonstrate that the addition of elliptic membership functions in the TSK fuzzy system, both with and without static feedforward control, offers superior performance compared to general TSK fuzzy-based PID control. Moreover, the proposed approach significantly outperforms conventional PID control. Notably, the integration of feedforward control resulted in a performance improvement that was approximately twice as high as that achieved by the system without feedforward, when compared to conventional PID control. Detailed explanations of performance indices are written in [2][16]. Among the reported performance indices, the ISE and ITAE are particularly indicative of disturbance-recovery performance, as both accumulate the tracking error that persists during the recovery transient following each door-opening event. A controller that recovers faster and with smaller residual error, therefore yields lower ISE and ITAE values.

Figure 3 illustrates the setpoint tracking performance of the system. While the addition of static feedforward control did not completely eliminate disturbances, it notably reduced the recovery time of the temperature control system by approximately 12 sampling instances, or 72 s faster, compared to the system without feedforward control. On the other hand, Figure 4 shows a comparison of the controller outputs. The controller with the additional static feedforward control maintained its 100 % duty cycle for several sampling instances to counteract the effects of periodic door openings in the industrial heating oven. Finally, Figure 5 depicts the time evolution of the PID gains, which showed almost identical trajectories across the different adaptive PID controllers, further validating the consistency and effectiveness of the proposed control approach.

B. Experimental validation

Building on the superior performance of the TSK elliptic fuzzy control observed in simulation results, this section aims to further validate the applicability and effectiveness of the proposed control strategy through experimental testing. Specifically, an experimental validation was conducted, targeting the issue of periodic door openings in an industrial heating oven. In this experiment, the conditions used in the simulation studies are carefully replicated to ensure a consistent comparison. This includes maintaining the same starting temperature, identical ambient conditions, and precisely timed door openings across all trials. Two different feedforward control gains were tested: $K_{FF} = 10$ and $K_{FF} = 15$, with all other parameters kept identical to those used in the prior simulation study.

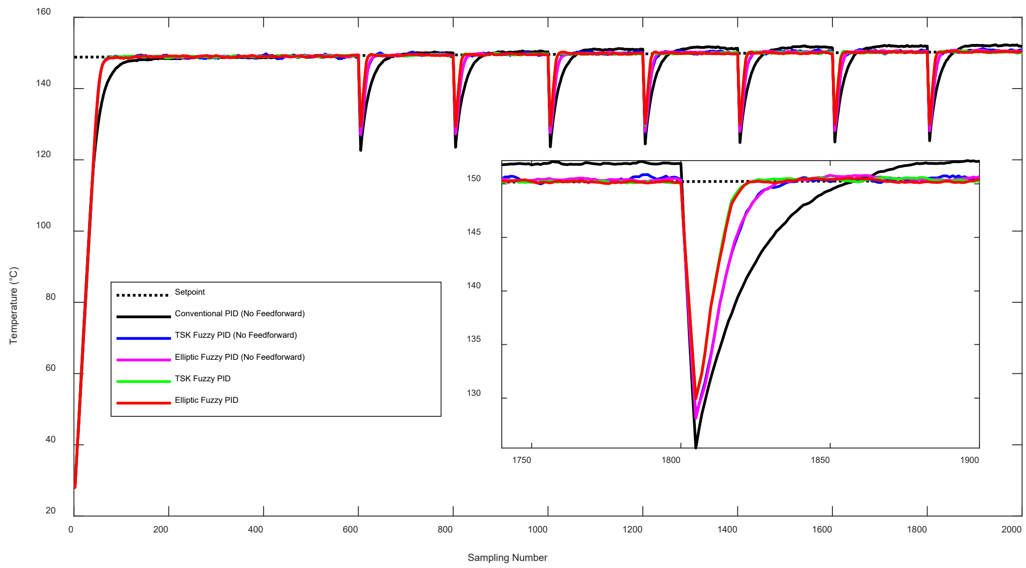

Figure 3. Comparison of simulated system output y for the five controllers.

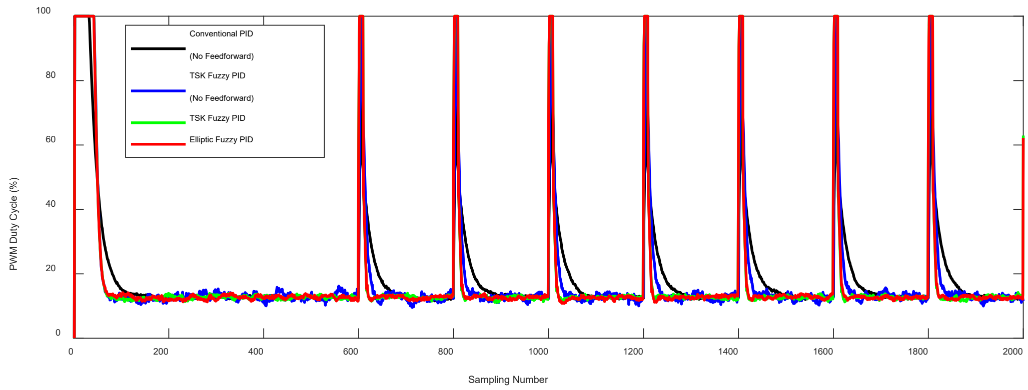

Figure 4. Comparison of simulated controllers output u for five controllers.

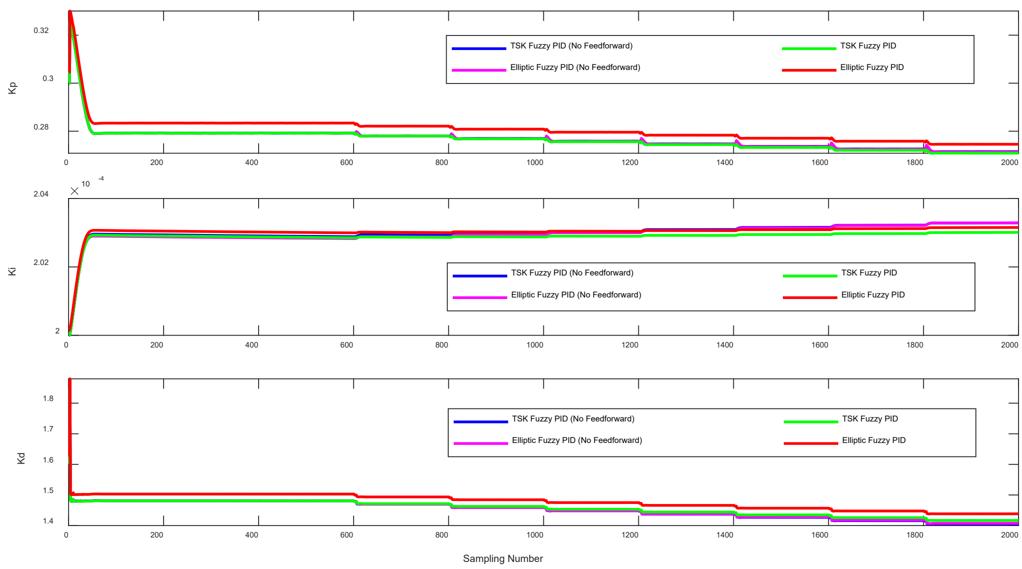

Figure 5. Simulation result for the PID gains evolution over time.

The results, shown in Figure 6, indicate that increasing the gain value K_{FF} leads to faster recovery times. Specifically, the system with $K_{FF} = 15$ exhibited a quicker recovery, with a temperature drop to 133.25 °C compared to 131 °C for $K_{FF} = 10$. This demonstrates that a higher gain not only reduces the temperature drop but also accelerates the recovery process. However, it is important to note that a higher

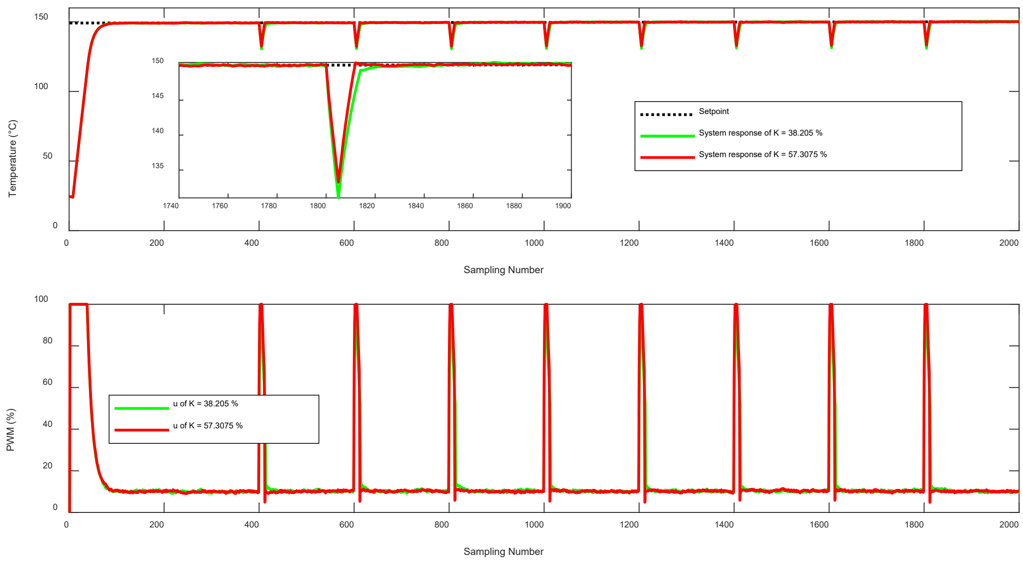

Figure 6. Experimental result of setpoint tracking and controller output for two feedforward settings, where $K = 38.205$ % corresponds to $K_{FF} = 10$ and $K = 57.3075$ % to $K_{FF} = 15$.

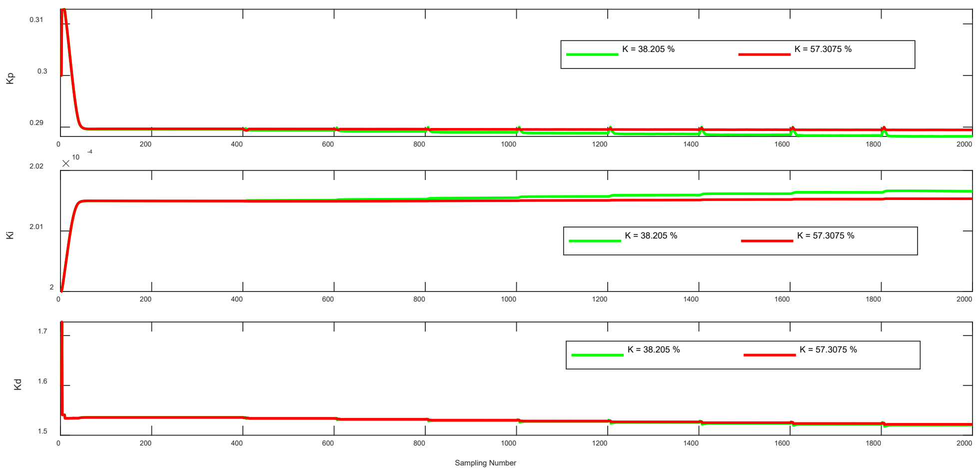

Figure 7. Experimental PID gain evolution over time for two feedforward settings, where $K = 38.205$ % corresponds to $K_{FF} = 10$ and $K = 57.3075$ % to $K_{FF} = 15$.

gain also increases the risk of overshot. In terms of recovery time, the configuration with $K_{FF} = 15$ recovered two sampling instances faster than the configuration with $K_{FF} = 10$. The controller output trajectories for both gains were nearly identical, with $K_{FF} = 15$, maintaining a 100 % duty cycle for three sampling instances, compared to just one instance for $K_{FF} = 10$. The evolution of the PID gains for both feedforward gain settings is depicted in Figure 7, where the trajectories appear almost identical, further supporting the consistency and effectiveness of the control strategy across different gain settings.

IV. Conclusion

This paper has presented a static feedforward control strategy combined with a TSK elliptic fuzzy-based adaptive PID controller for temperature regulation in industrial heating ovens subject to observable disturbances such as periodic door openings. The approach was validated through both simulation and experiment on an STM32 microcontroller. Compared with a conventional PID controller, the proposed method reduced the RMSE by 32.27 % and the ISE by 54.13 %, while shortening the temperature recovery time by approximately 72 s. The static feedforward path, activated directly by the door-state signal, was primarily responsible for the faster recovery and the reduced temperature drop. The TSK elliptic fuzzy-based adaptive PID maintained stability and tuned the gains online, and the elliptic membership function, with its wider support, handled the nonlinearity and measurement noise of the thermal process more smoothly than the standard TSK fuzzy form, giving lower error indices in both simulation and experiment. Experimental results further confirmed these findings, with a higher feedforward gain yielding a smaller temperature drop and faster recovery, at a slight risk of overshoot. Future work could extend the strategy to other thermal processes and disturbance types, and incorporate online gain optimization or learning-based disturbance prediction to further enhance robustness.

Acknowledgements

A. Rospawan acknowledges financial support from the Directorate General of Higher Education, Ministry of Higher Education, Science, and Technology, Republic of Indonesia.

Declarations

Author contribution

A. Rospawan: Methodology, Formal Analysis, Writing – Original Draft. **C.L. Angelina**: Methodology, Writing – Review & Editing, Project Administration. **I.M.A. Setiawan**: Formal Analysis, Supervision. **Z. Saputra**: Formal Analysis, Validation. **Ocsirendi**: Software, Validation. **A. Febriansyah**: Supervision, Writing – Review & Editing. **I. Dwisaputra**: Investigation, Software. **D.R. Harahap**: Validation, Writing – Review & Editing.

Funding statement

This research did not receive any specific grant from funding agencies in the public, commercial, or not-for-profit sectors.

Competing interests

The authors declare that they have no known competing financial interests or personal relationships that could have appeared to influence the work reported in this paper.

The use of AI or AI-assisted technologies

During the preparation of this work the authors used CLAUDE in order to check grammar and language clarity. After using this tool/service, the authors reviewed and edited the content as needed and takes full responsibility for the content of the publication.

Additional information

Reprints and permission: information is available at https://mev.brin.go.id/.

Publisher's Note: National Research and Innovation Agency (BRIN) remains neutral with regard to jurisdictional claims in published maps and institutional affiliations.

References

[1] N. Wang *et al.*, "High efficiency thermoelectric temperature control system with improved proportional integral differential algorithm using energy feedback technique," *IEEE Trans. Ind. Electron.*, vol. 69, no. 5, pp. 5225–5234, May 2022.

[2] A. Rospawan, C. C. Tsai, and C. C. Hung, "Output recurrent fuzzy broad learning systems for adaptive MIMO PID control: theory, simulations, and application," *IEEE Access*, vol. 12, pp. 19388–19404, 2024.

[3] J. Hao, G. Zhang, W. Liu, Y. Zheng, and L. Ren, "Data-driven tracking control based on LM and PID neural network with relay feedback for discrete nonlinear systems," *IEEE Transactions on Industrial Electronics*, vol. 68, no. 11, pp. 11587–11597, Nov. 2021.

[4] Y. Hou, "Adaptive virtual impedance control strategy based on IWOA-fuzzy PID and its application to reactive power sharing in islanded microgrids," *Scientific Reports*, vol. 16, no. 1, p. 2833, Dec. 2025.

[5] J. S. Saputro *et al.*, "Design of intelligent cruise control system using fuzzy-PID control on autonomous electric vehicles prototypes," *Journal of Mechatronics, Electrical Power, and Vehicular Technology*, vol. 15, no. 1, pp. 105–116, Jul. 2024.

[6] P. Kaliappan, A. Ilangovan, S. Muthusamy, and B. Sembanan, "Temperature control design with differential evolution based improved adaptive-fuzzy-PID techniques," *Intelligent Automation & Soft Computing*, vol. 36, no. 1, pp. 781–801, 2022.

[7] M. Liu, L. Cheng, J. Xu, X. Zhang, and H. Zhang, "An improved particle swarm fuzzy PID for adaptive control of temperature in CFRP induction heating," *Proceedings of the Institution of Mechanical Engineers, Part B: Journal of Engineering Manufacture*, vol. 238, no. 4, pp. 500–513, Mar. 2024.

[8] B. Ghosh and S. Mandal, "Enhanced solar PV cell parameter identification via particle swarm optimization (PSO) with weighted objective function," *Journal of Mechatronics, Electrical Power, and Vehicular Technology*, vol. 16, no. 1, pp. 15–26, Jun. 2025.

[9] S. Asgari, A. A. Suratgar, and M. Kazemi, "Feedforward fractional order PID load frequency control of microgrid using harmony search algorithm," *Iranian Journal of Science and Technology, Transactions of Electrical Engineering*, vol. 45, no. 4, pp. 1369–1381, Dec. 2021.

[10] Z. Bingul and K. Gul, "Intelligent-PID with PD Feedforward Trajectory Tracking Control of an Autonomous Underwater Vehicle," *Machines*, vol. 11, no. 2, Art. no. 2, Feb. 2023.

[11] Z. Liu, H. Chen, L. Peng, X. Ye, S. Xu, and T. Zhang, "Feedforward-decoupled closed-loop fuzzy proportion-integral-derivative control of air supply system of proton exchange membrane fuel cell," *Energy*, vol. 240, p. 122490, Feb. 2022.

[12] H. Yuan, H. Dai, W. Wu, J. Xie, J. Shen, and X. Wei, "A fuzzy logic PI control with feedforward compensation for hydrogen pressure in vehicular fuel cell system," *International Journal of Hydrogen Energy*, vol. 46, no. 7, pp. 5714–5728, Jan. 2021.

[13] D. H. Pham, C. M. Lin, V. N. Giap, V. P. Vu, and H. Y. Cho, "Design of missile guidance law using Takagi-Sugeno-Kang (TSK) elliptic type-2 fuzzy brain imitated neural networks," *IEEE Access*, vol. 11, pp. 53687–53702, 2023.

[14] D.-H. Pham, C.-M. Lin, V.-N. Giap, V.-T. Nguyen, and N.-T. Pham, "Self-organizing Takagi–Sugeno–Kang fuzzy elliptic type-2 CMAC for nonlinear systems with uncertainty," *Int. J. Fuzzy Syst.*, May 2025.

[15] A. Rospawan, C. C. Tsai, and C. C. Hung, "Two-layer intelligent learning control using output recurrent fuzzy neural long short-term memory broad learning system with RMSprop," *IEEE Access*, vol. 13, pp. 34334–34349, Feb. 2025.

[16] I. I. Novendra *et al.*, "Optimization of load frequency control using grey wolf optimizer in micro hydro power plants," *Journal of Mechatronics, Electrical Power, and Vehicular Technology*, vol. 14, no. 2, pp. 166–176, Dec. 2023.

[17] A. Rospawan, C. C. Tsai, and C. C. Hung, "Intelligent MIMO ORFBLS-based setpoint tracking control with its application to temperature control of an industrial extrusion barrel," *International Journal of Fuzzy Systems*, vol. 27, no. 3, pp. 774–790, Jun. 2024.

[18] K. A. Metwally *et al.*, "Drying kinetics, power consumption, economic and environmental analysis of pomegranate peels drying using a hybrid solar dryer compared with oven dryer," *Scientific Reports*, vol. 16, no. 1, p. 7395, Feb. 2026.

[19] J. Meng, W. Sun, Q. F. Pan, and M. X. Ruan, "Research and application of improved particle swarm fuzzy PID algorithm based on self- disturbance rejection in temperature control system of plastic extruder," *IEEE Access*, vol. 12, pp. 41620–41630, 2024.

[20] A. Rospawan *et al.*, "Adaptive nonlinear PID control of DC motor position using a polynomial fuzzy long short-term memory neural network," *International Journal of Automotive and Mechanical Engineering*, vol. 22, no. 3, pp. 12821–12836, Oct. 2025.

[21] T. Wang, R. Gault, and D. Greer, "Ensemble learning-based fuzzy aggregation functions and their application in TSK neural networks," *Int. J. Fuzzy Syst.*, vol. 27, no. 4, pp. 1115–1126, Jun. 2025.

[22] A. Rospawan *et al.*, "Direct control strategy using polynomial fuzzy-based adaptive fractional order PID controller," *Makara Journal of Technology*, vol. 29, no. 2, Aug. 2025.

[23] V.-T. Nguyen, D.-N. Duong, D.-H. Pham, V.-T. Ngo, and L. A. Tuan, "Optimal nonlinear PID TSK3DCMAC controller based on balancing composite motion optimization for ballbot with external forces," *ISA Transactions*, vol. 158, pp. 654–673, Mar. 2025.

[24] C. C. Tsai, C. C. Hung, C. F. Mao, H. S. Wu, and C. H. Chen, "Fuzzy neural LSTM-RBLS for fractional-order PID sliding-mode motion control of autonomous mobile robots with four ISID wheels," *Int. J. Fuzzy Syst.*, vol. 27, pp. 2195–2213, 2025.

[25] N. Querejeta, S. García, N. Álvarez-Gutiérrez, F. Rubiera, and C. Pevida, "Measuring heat capacity of activated carbons for CO2 capture," *Journal of CO2 Utilization*, vol. 33, pp. 148–156, Oct. 2019.

[26] M. Ma, L. Qian, Y. Zhang, Q. Fang, and G. Xue, "An adaptive double-parameter softmin based Takagi-Sugeno-Kang fuzzy system for high-dimensional data," *Fuzzy Sets and Systems*, vol. 521, p. 109582, Dec. 2025.